Nr. 25
11. July 2016

Leopold-Franzens-Universität Innsbruck

Preprint-Series: Department of Mathematics - Applied Mathematics

The Radon Transform over Cones with Vertices on the Sphere and Orthogonal Axes

Daniela Schiefeneder, Markus Haltmeier

Technikerstraße 13 - 6020 Innsbruck - Austria
Tel.: +43 512 507 53803 Fax: +43 512 507 53898
https://applied-math.uibk.ac.at

The Radon Transform over Cones with Vertices on the Sphere and Orthogonal Axes

Daniela Schiefeneder and Markus Haltmeier

Department of Mathematics, University of Innsbruck
Technikerstrasse 13, A-6020 Innsbruck, Austria
{Daniela.Schiefeneder,Markus.Haltmeier}@uibk.ac.at

Abstract

Recovering a function from its integrals over circular cones recently gained significance because of its relevance to novel medical imaging technologies such emission tomography using Compton cameras. In this paper we investigate the case where the vertices of the cones of integration are restricted to a sphere in n-dimensional space and symmetry axes are orthogonal to the sphere. We show invertibility of the considered transform and develop an inversion method based on series expansion and reduction to a system of one-dimensional integral equations of generalized Abel type. Because the arising kernels do not satisfy standard assumptions, we also develop a uniqueness result for generalized Abel equations where the kernel has zeros on the diagonal. Finally, we demonstrate how to numerically implement our inversion method and present numerical results.

Keywords: Computed tomography; Radon transform; SPECT; Compton cameras; conical Radon transform; uniqueness of reconstruction; spherical harmonics decomposition; series expansion; generalized Abel equations; first kind Volterra equations with zeros in diagonal.

AMS Subject Classification: 44A12, 45D05, 92C55.

1 Introduction

Many tomographic imaging modalities are based on the inversion of Radon transforms, which map a function onto its integrals over certain surfaces in $\mathbb{R}^n$ (see, for example, [23, 31]). The most basic example is the classical Radon transform which maps the function onto its integrals over hyperplanes and which is the mathematical basis of X-ray CT. Another well investigated example is the spherical Radon transform, which maps a function onto its integrals over hyper-spheres and which finds application in the recently developed photoacoustic tomography [13, 14, 24]. In this article we consider the conical Radon transform that maps a function to its integrals over circular half cones. The conical Radon transform recently

gained increased interest, mainly due to its relevance for SPECT using Compton cameras (see, for example, [1, 6, 8, 19, 21, 28, 29, 33, 38, 42]).

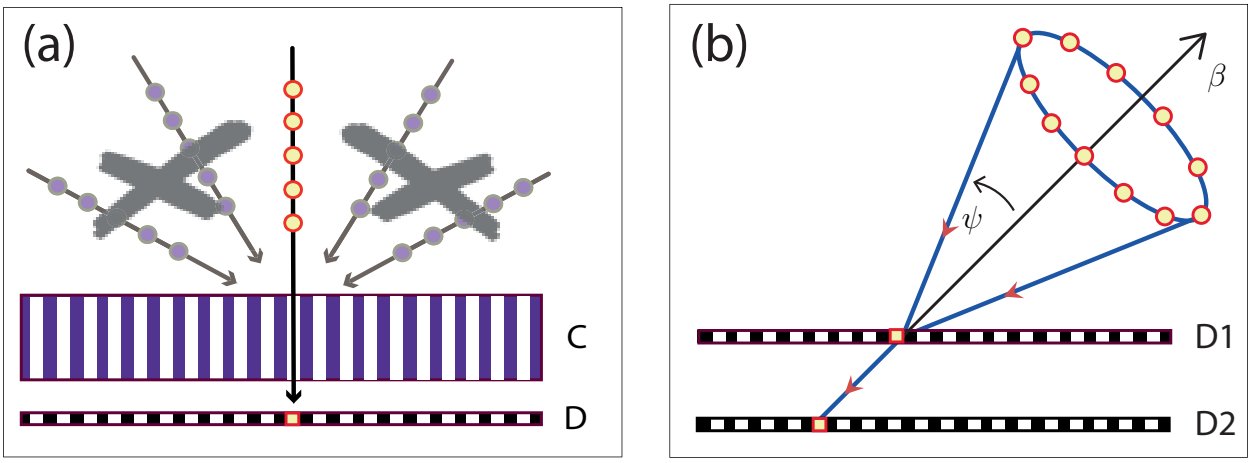

Figure 1: (a) Standard gamma cameras use collimators which only observe photons propagating orthogonal to the detector plane. The location of emitted photons can be traced back to a straight line. (b) A Compton camera consists of two detector arrays and any observed photon can be traced back to the surface of a cone.

1.1 SPECT using Compton cameras

Single-photon emission computed tomography (SPECT) is a well established medical imaging technology for functional imaging. In SPECT, weakly radioactive tracers are given to patient and participate in the physiological processes. The radioactive tracers can be detected through the emission of gamma ray photons which provide information about the interior of patient. In order to obtain location information on the emitted photons, the standard approach in SPECT uses collimators which only record photons that enter the detector vertically. As illustrated in Figure 1(a), such data provide values of line integrals of the tracer distribution.

A major drawback of using collimators is that they remove most photons. Therefore the number of recorded photons is low and the noise level high. Typically, only one out of 10 000 photons emitted from the patient is actually detected with this standard approach. In order to increase the number of recorded photons, the concept of Compton cameras has been developed in [11, 37, 41]. As illustrated in Figure 1(b), a Compton camera consists of a scatter detector array D1 and an absorption detector array D2. A photon emitted in the direction of the camera undergoes Compton scattering in D1, and is absorbed in D2. The required distinction of individual photons is obtained by coincidence detection. Both detectors are position and energy sensitive, and the measured energies can be used to determine the scattering angle [37]. Using such information, one concludes that the detected photon must have been emitted on the surface of a circular cone, where the vertex is given by the position at D1, the central axis points from the position on D2 to the position on D1, and the opening angle equals the Compton scattering angle. Consequently, for a distribution

of tracers, the Compton camera approximately provides integrals of the marker distribution over conical surfaces.

1.2 Inversion of the conical Radon transform

As outlined above, SPECT with Compton cameras yields to the conical Radon transform that maps a function $f\colon \mathbb{R}^3 \to \mathbb{R}$ modeling the marker distribution to the surface integrals $\int_{C(z,\beta,\psi)} f \,\mathrm{d}S$ over right circular half cones

$$C(z,\beta,\psi) = \{z + r\omega \mid r \geq 0 \text{ and } \omega \in \mathbb{S}^2 \text{ with } \omega \bullet \beta = \cos\psi\}\,.$$

Here $z \in \mathbb{R}^3$ is the vertex of the cone, $\beta \in \mathbb{S}^2$ the direction of the central axis, and $\psi \in (0, \pi/2)$ the half opening angle. Variants of the conical Radon transform in $\mathbb{R}^2$ are known as V-line or broken-ray transforms. These transforms appear in emission tomography with one-dimensional Compton cameras [5, 22], or in the recently developed single scattering optical tomography [16]. In this paper, we consider the conical Radon transform in general dimension and further include a radial weight, that can be adjusted to a particular application at hand. In previous work on Compton camera imaging [38], models with and without radial weight have been proposed and used.

The conical Radon transform depends on six parameters $(z,\beta,\psi) \in \mathbb{R}^3 \times \mathbb{S}^2 \times (0,\pi/2)$, whereas the function f only depends on three spatial coordinates. Therefore the problem of reconstructing f from its integrals over all circular cones is highly overdetermined. Several authors have studied the problem of inverting the function from integrals over particular subsets of all cones. In SPECT with Compton cameras, the vertex is naturally fixed to the scattering surface D1. In the case where D1 is a plane and the axis is fixed to $\beta = (1,0,0)$, Fourier reconstruction formulas have been derived in [8, 32]. Formulas of the filtered backprojection type have been derived in [19, 28]. The case of variable axis and vertices restricted to a surface has been considered in [6, 21, 27, 33, 38, 39, 42]. See also [1, 3, 15, 17] for related results on different conical transforms.

To the best of our knowledge, if the set of vertices is different from a plane and any vertex is associated with a single symmetry axis, no results are known for reconstructing a function from its integrals over such cones. In this paper we develop an inversion approach for the case when $D1$ is a sphere and the symmetry axes of the cones are orthogonal to the sphere. We derive a reconstruction procedure based on spherical harmonics decomposition and show invertibility of the considered transform. Spherical harmonics decompositions have been previously used for studying other Radon transforms. See, for example, [7, 9, 26, 31] for the classical Radon transform, [35] for a weighted Radon transform over planes, [2] for the circular Radon transform, or [3, 4] for a broken ray transform with vertices in a disc. In these works, the arising generalized Abel equations satisfy all conditions needed in order to apply standard well-posedness results. For the transform we study, one basic assumption of these results is violated, namely the kernels turn out to have zeros on the diagonal (see Theorem 3.2). Nevertheless, we are able to show solution uniqueness; see Theorem 3.5.

1.3 Outline

The paper is organized as follows. In Section 2 we define the conical Radon transform with vertices on the sphere and orthogonal axis, and derive some elementary results for that transform. Our main results are stated in Section 3. By using expansions in spherical harmonics, we are able the reduce the conical Radon transform to a set of explicitly given one-dimensional integral equations of the Abel type (see Theorem 3.2). The invertibility of the one dimensional integral operators will be given in Theorem 3.5. For that purpose, in Appendix A we derive uniqueness results for first kind Volterra equations (Theorem A.2) and generalized Abel equations with kernels having zeros on the diagonal (Theorem 3.4). Theorem 3.5 in particular implies injectivity of the considered transform and additionally yields an efficient inversion method. In Section 4, we develop such a reconstruction procedure based on our theoretical findings and present some numerical results. Finally, in Section 5 we present a short summary and discuss possible lines of future research.

2 The conical Radon transform

We start this section with defining the conical Radon transform that integrates a function over cones with vertices on the unit sphere $\mathbb{S}^{n-1} = \{x \in \mathbb{R}^n \mid \|x\| = 1\}$ and central axis orthogonal to $\mathbb{S}^{n-1}$. For $z \in \mathbb{S}^{n-1}$ and $\psi \in (0, \pi/2)$, we denote by

$$C(z,\psi) = \{z + r\omega \mid r \geq 0 \text{ and } \omega \in \mathbb{S}^{n-1} \text{ with } -\omega \bullet z = \cos\psi\},$$

the surface of a right circular half cone in $\mathbb{R}^n$ with vertex z, central axis $-z$ and half opening angle ψ. We denote by $C_0^\infty(B_1(0))$ the set of all infinitely times differentiable functions $f\colon \mathbb{R}^n \to \mathbb{R}$ with $\operatorname{supp}(f) \subseteq B_1(0)$, where $B_1(0) \coloneqq \{x \in \mathbb{R}^n \mid \|x\| < 1\}$ denotes the unit ball in $\mathbb{R}^n$. Further, we denote by $O(n) \subseteq \mathbb{R}^{n\times n}$ the set of all orthogonal $n \times n$ matrices and set $e_1 \coloneqq (1, 0, \ldots, 0)$.

Definition 2.1 (The conical Radon transform $\mathcal{R}_m f$)**.** Let $m \in \mathbb{Z}$. We define the conical Radon transform (with vertices on the sphere, orthogonal axis and weighting factor m) of $f \in C_0^\infty(B_1(0))$ by

$$\mathcal{R}_m f\colon \mathbb{S}^{n-1} \times (0, \pi/2) \to \mathbb{R}\colon (z,\psi) \mapsto \int_{C(z,\psi)} f(x)\, \|x - z\|^m \,\mathrm{d}S(x)\,. \tag{2.1}$$

The problem under study is recovering the function f from its conical Radon transform $\mathcal{R}_m f$. We start by deriving explicit expressions for $\mathcal{R}_m f$.

Lemma 2.2. *Let $m \in \mathbb{Z}$ and $f \in C_0^\infty(B_1(0))$.*

(a) If $Q \in O(n)$ and $z \in \mathbb{S}^{n-1}$, then $(\mathcal{R}_m f)(Qz, \cdot) = \mathcal{R}_m(f \circ Q)(z, \cdot)$.

(b) For every $(z,\psi) \in \mathbb{S}^{n-1} \times (0, \pi/2)$, we have

$$(\mathcal{R}_m f)(e_1, \psi) = \int_0^2 r^m (r\sin(\psi))^{n-2} \tag{2.2}$$

$$\times \int_{\mathbb{S}^{n-2}} f(1 - r\cos(\psi), r\sin(\psi)\eta)\,\mathrm{d}S(\eta)\,\mathrm{d}r\,,$$

$$(\mathcal{R}_m f)(e_1,\psi) = \int_0^{\pi-\psi} \frac{(\sin(\psi))^{n-1}(\sin(\alpha))^{m+n-2}}{(\sin(\alpha+\psi))^{m+n}} \tag{2.3}$$

$$\times \int_{\mathbb{S}^{n-2}} f\left(\frac{\sin(\psi)}{\sin(\alpha+\psi)}(\cos(\alpha), \sin(\alpha)\eta)\right)\mathrm{d}S(\eta)\,\mathrm{d}\alpha\,.$$

Proof. (a) For every $Q \in O(n)$ and every $(z,\psi) \in \mathbb{S}^{n-1} \times (0,\pi/2)$, we have

$$\begin{aligned}
(\mathcal{R}_m f)(Qz,\psi) &= \int_{C(Qz,\psi)} f(x)\|x - Qz\|^m\,\mathrm{d}S(x)\\
&= \int_{Q(C(z,\psi))} f(x)\|x - Qz\|^m\,\mathrm{d}S(x)\\
&= \int_{C(z,\psi)} f(Q\,x)\|Q\,x - Qz\|^m\,\mathrm{d}S(x)\\
&= \int_{C(z,\psi)} (f\circ Q)(x)\|x - z\|^m\,\mathrm{d}S(x)\\
&= \mathcal{R}_m(f\circ Q)(z,\psi).
\end{aligned}$$

(b) Let $\Phi\colon D \to \mathbb{R}^{n-1}$ be any parametrization of $\mathbb{S}^{n-2}$, where $D \subseteq \mathbb{R}^{n-2}$ is an open subset of $\mathbb{R}^{n-2}$. Then

$$\Psi\colon D\times(0,\infty) \to \mathbb{R}^n\colon (r,\beta) \mapsto (1 - r\cos(\psi), r\sin(\psi)\Phi(\beta))$$

is a parametrization of $C(e_1,\psi)$. Elementary computation shows that the Gramian determinant of Ψ is given by $\det(\Psi'(r,\beta)^{\mathsf{T}}\Psi'(r,\beta)) = (r\sin\psi)^{2(n-2)}\det(\Phi'(\beta)^{\mathsf{T}}\Phi'(\beta))$. Consequently,

$$\begin{aligned}
(\mathcal{R}_m f)(e_1,\psi) &= \int_{C(e_1,\psi)} f(x)\,\|x - e_1\|^m\,\mathrm{d}S(x)\\
&= \int_0^\infty r^m(r\sin(\psi))^{n-2}\int_D f\,(1 - r\cos(\psi), r\sin(\psi)\Phi(\beta))\\
&\qquad\qquad \times\sqrt{\det(\Phi'(\beta)^T\Phi'(\beta))}\,\mathrm{d}\beta\,\mathrm{d}r\\
&= \int_0^\infty r^m(r\sin(\psi))^{n-2}\int_{\mathbb{S}^{n-2}} f\,(1 - r\cos(\psi), r\sin(\psi)\eta)\,\mathrm{d}S(\eta)\,\mathrm{d}r\,,
\end{aligned}$$

which is (2.2). Substituting $r = \sin(\alpha)/\sin(\alpha+\psi)$, we have $\mathrm{d}r/\,\mathrm{d}\alpha = \sin(\psi)(\sin(\alpha+\psi))^{-2}$ and $1 - r\cos(\psi) = \cos(\alpha)\sin(\psi)/\sin(\alpha+\psi)$; this yields (2.3). □

Next we state the continuity of $f \mapsto \mathcal{R}_m f$ with respect to the L^p-norms for $p \in \{1,2\}$. Similar results could of course be obtained for any $p \in [1,\infty)$.

Lemma 2.3 (Continuity of $\mathcal{R}_m$)**.** *Let $m \in \mathbb{Z}$, $f \in C_0^\infty(B_1(0))$ and $\epsilon \in (0,1)$.*

(a) If $2m+n-2 > 0$, then $\|\mathcal{R}_m f\|_{L^2} \le \frac{|\mathbb{S}^{n-1}||\mathbb{S}^{n-2}|\ 2^{2m+n-2}}{2m+n-2}\|f\|_{L^2}$.

(b) If $m \geq 1$, then $\|\mathcal{R}_m f\|_{L^1} \leq 2^m \|f\|_{L^1}$.

(c) If $\operatorname{supp}(f) \subseteq B_{1-\epsilon}(0)$, then $\|\mathcal{R}_m f\|_{L^1} \leq C^{(1)}_{\epsilon,m} \|f\|_{L^1}$, $\|\mathcal{R}_m f\|_{L^2} \leq C^{(2)}_{\epsilon,m} \|f\|_{L^2}$ for constants $C^{(1)}_{\epsilon,m}$ and $C^{(2)}_{\epsilon,m}$ independent of f.

Proof. (a) Let $z \in \mathbb{S}^{n-2}$ and $Q \in O(n)$ satisfy $Qe_1 = z$. By Lemma 2.2, we have

$$\|(\mathcal{R}_m f)(z, \cdot)\|^2_{L^2} = \int_0^{\pi/2} |\mathcal{R}_m(f \circ Q)(e_1, \psi)|^2 \, \mathrm{d}\psi = \int_0^{\pi/2} (\sin(\psi))^{2(n-2)} \times \left| \int_0^2 r^{m+n-2} \int_{\mathbb{S}^{n-2}} (f \circ Q)\,(1 - r\cos(\psi), r\sin(\psi)\eta) \, \mathrm{d}S(\eta) \, \mathrm{d}r \right|^2 \mathrm{d}\psi \,.$$

Using the Cauchy-Schwarz inequality, we obtain

$$\|(\mathcal{R}_m f)(z, \cdot)\|^2_{L^2} \leq |\mathbb{S}^{n-2}| \left(\int_0^2 r^{2m+n-3} \, \mathrm{d}r \right) \left(\int_0^{\pi/2} (\sin(\psi))^{2(n-2)} \times \int_0^2 \int_{\mathbb{S}^{n-2}} r^{n-1} |(f \circ Q)\,(1 - r\cos(\psi), r\sin(\psi)\eta)|^2 \, \mathrm{d}S(\eta) \, \mathrm{d}r \, \mathrm{d}\psi \right).$$

The first integral equals $\int_0^2 r^{2m+n-3} \, \mathrm{d}r = 2^{2m+n-2}/(2m+n-2)$, and the second can be bounded by $\|f\|^2_{L^2}$. Consequently, $\|(\mathcal{R}_m f)(z, \cdot)\|^2_{L^2} \leq |\mathbb{S}^{n-2}| \, 2^{2m+n-2}/(2m+n-2) \|f\|^2_{L^2}$. Integration over $z \in \mathbb{S}^{n-1}$ yields the claimed estimate.

(b), (c): Analogous to (a). □

3 Analytic inversion of $\mathcal{R}_m$

In this section, first we derive an explicit decomposition of the conical Radon transform in one-dimensional integral operators (see Theorem 3.2). Second, we show the solution uniqueness of the corresponding generalized Abel equations (see Theorem 3.5), which implies the invertibility of $\mathcal{R}_m$. For these results we will use the spherical harmonic decompositions

$$f(r\theta) = \sum_{\ell=0}^{\infty} \sum_{k=1}^{N(n,\ell)} f_{\ell,k}(r) \, Y_{\ell,k}(\theta) \,, \tag{3.1}$$

$$(\mathcal{R}_m f)(z, \psi) = \sum_{\ell=0}^{\infty} \sum_{k=1}^{N(n,\ell)} (\mathcal{R}_m f)_{\ell,k}(\psi) Y_{\ell,k}(z) \,. \tag{3.2}$$

Here $Y_{\ell,k}$, for $\ell \in \mathbb{N}$ and $k \in \{1, \ldots, N(n,\ell)\}$, denote spherical harmonics [30, 36] of degree ℓ forming a complete orthonormal system in $\mathbb{S}^{n-1}$. The set of all (ℓ, k) with $\ell \in \mathbb{N}$ and $k \in \{1, \ldots, N(n,\ell)\}$ will be denoted by $I(n)$.

3.1 Integral equations for $f_{\ell,k}$

Let C_ℓ^μ denote the Gegenbauer polynomials normalized in such a way that $C_\ell^\mu(1) = 1$. We derive three different relations between $f_{\ell,k}$ and $(\mathcal{R}_m f)_{\ell,k}$. The first one is as follows.

Lemma 3.1. *Let $f \in C_0^\infty(B_1(0))$, and let $f_{\ell,k}$ and $(\mathcal{R}_m f)_{\ell,k}$ for $(\ell,k) \in I(n)$ be as in (3.1) and (3.2). Then*

$$\forall \psi \in (0,\pi/2): \quad (\mathcal{R}_m f)_{\ell,k}(\psi) = |\mathbb{S}^{n-2}| \int_0^{\pi-\psi} f_{\ell,k}\left(\frac{\sin(\psi)}{\sin(\alpha+\psi)}\right) \times \frac{(\sin(\psi))^{n-1}(\sin(\alpha))^{m+n-2}}{(\sin(\alpha+\psi))^{m+n}} C_\ell^{(n-2)/2}(\cos(\alpha))\,\mathrm{d}\alpha\,. \quad (3.3)$$

Proof. Fix $z \in \mathbb{S}^{n-1}$ and let $Q \in O(n)$ be any rotation with $Qe_1 = z$. Using the delta distribution δ and applying the Funk-Hecke theorem, for any $\alpha \in (0,\pi)$ we have

$$\begin{aligned}
&\int_{\mathbb{S}^{n-2}} Y_{\ell,k}(Q(\cos(\alpha), \sin(\alpha)\eta))\,\mathrm{d}S(\eta) \\
&\qquad = \int_{\mathbb{S}^{n-1}} Y_{\ell,k}\left(Q\eta\right)\, \delta(e_1 \bullet \eta - \cos(\alpha))\,(1-(e_1\bullet\eta)^2)^{-(n-3)/2}\,\mathrm{d}S(\eta) \\
&\qquad = \int_{\mathbb{S}^{n-1}} Y_{\ell,k}(\eta)\,\delta(z\bullet\eta - \cos(\alpha))\,(1-(z\bullet\eta)^2)^{-(n-3)/2}\,\mathrm{d}S(\eta) \\
&\qquad = |\mathbb{S}^{n-2}|\, Y_{\ell,k}(z) \int_{-1}^{1} \delta(t-\cos(\alpha)) C_\ell^{(n-2)/2}(t)\,\mathrm{d}t \\
&\qquad = |\mathbb{S}^{n-2}|\, Y_{\ell,k}(z)\, C_\ell^{(n-2)/2}(\cos(\alpha))\,.
\end{aligned} \quad (3.4)$$

Together with Lemma 2.2, this yields

$$\mathcal{R}_m[x \mapsto f_{\ell,k}(|x|)\,Y_{\ell,k}(x/|x|)](z,\psi) = |\mathbb{S}^{n-2}| \left(\int_0^{\pi-\psi} f_{\ell,k}\left(\frac{\sin(\psi)}{\sin(\alpha+\psi)}\right) \times \frac{(\sin(\psi))^{n-1}(\sin(\alpha))^{m+n-2}}{(\sin(\alpha+\psi))^{m+n}}\, C_\ell^{(n-2)/2}(\cos(\alpha))\,\mathrm{d}\alpha \right) Y_{\ell,k}(z)\,.$$

The linearity of $\mathcal{R}_m$ gives (3.3). ∎

Theorem 3.2 (Generalized Abel equation for $f_{\ell,k}$)**.** *Let $f \in C_0^\infty(B_1(0))$ and let $f_{\ell,k}$ and $(\mathcal{R}_m f)_{\ell,k}$ be as (3.1) and (3.2) for $(\ell,k) \in I(n)$. Then, for $\psi \in (0,\pi/2)$,*

$$(\mathcal{R}_m f)_{\ell,k}(\psi) = |\mathbb{S}^{n-2}|\,\sin(\psi)^{-m} \int_{\sin(\psi)}^1 f_{\ell,k}(\rho) \frac{\rho\, K_\ell(\psi,\rho)}{\sqrt{\rho^2 - (\sin(\psi))^2}}\,\mathrm{d}\rho\,, \quad (3.5)$$

with the kernel functions

$$K_\ell(\psi,\rho) := \rho^{m+n-2} \sum_{\sigma=\pm 1} \sigma^\ell \sin\left(\arcsin\left(\sin(\psi)/\rho\right) - \sigma\psi\right)^{m+n-2} \times C_\ell^{(n-2)/2}\left(\cos\left(\arcsin\left(\sin(\psi)/\rho\right) - \sigma\psi\right)\right)\,. \quad (3.6)$$

Proof. We split the integral in Lemma 3.1 in one integral over $\alpha < \pi/2 - \psi$ and one over $\alpha \geq \pi/2 - \psi$. For $\alpha < \pi/2 - \psi$ we substitute $\alpha = \arcsin(\sin(\psi)/\rho) - \psi$. We have $\mathrm{d}\alpha/\mathrm{d}\rho = -\sin(\psi)\,\rho^{-1}(\rho^2 - \sin(\psi)^2)^{-1/2}$ and therefore

$$\begin{aligned}
\int_0^{\pi/2-\psi} f_{\ell,k}\left(\frac{\sin(\psi)}{\sin(\alpha+\psi)}\right) \frac{(\sin(\psi))^{n-1}(\sin(\alpha))^{m+n-2}}{(\sin(\alpha+\psi))^{m+n}} C_\ell^{(n-2)/2}(\cos(\alpha))\,\mathrm{d}\alpha \\
&= (\sin(\psi))^{n-1} \int_{\sin\psi}^1 f_{\ell,k}(\rho)\, C_\ell^{(n-2)/2}\left(\cos\left(\arcsin\left(\sin(\psi)/\rho\right) - \psi\right)\right) \\
&\quad \times \left(\sin\left(\arcsin\left(\sin(\psi)/\rho\right) - \psi\right)\right)^{m+n-2} \frac{\rho^{m+n}}{\sin(\psi)^{m+n}} \frac{\sin(\psi)\,\mathrm{d}\rho}{\rho\sqrt{\rho^2 - (\sin(\psi))^2}} \\
&= (\sin(\psi))^{-m} \int_{\sin\psi}^1 f_{\ell,k}(\rho) C_\ell^{(n-2)/2}\left(\cos\left(\arcsin\left(\sin(\psi)/\rho\right) - \psi\right)\right) \\
&\quad \times \left(\sin\left(\arcsin\left(\sin(\psi)/\rho\right) - \psi\right)\right)^{m+n-2} \frac{\rho^{m+n-1}\,\mathrm{d}\rho}{\sqrt{\rho^2 - (\sin(\psi))^2}}\,.
\end{aligned}$$

In the case $\alpha > \pi/2 - \psi$, we substitute $\alpha = \pi - \arcsin\left(\sin(\psi)/\rho\right) - \psi$. Repeating the above computations and using $C_\ell^\mu(-x) = (-1)^\ell C_\ell^\mu(x)$ shows

$$\begin{aligned}
\int_{\pi/2-\psi}^{\pi-\psi} f_{\ell,k}\left(\frac{\sin(\psi)}{\sin(\alpha+\psi)}\right) \frac{(\sin(\psi))^{n-1}(\sin(\alpha))^{m+n-2}}{(\sin(\alpha+\psi))^{m+n}} C_\ell^{(n-2)/2}(\cos(\alpha))\,\mathrm{d}\alpha \\
&= (-1)^\ell (\sin(\psi))^{-m} \int_{\sin\psi}^1 f_{\ell,k}(\rho) C_\ell^{(n-2)/2}\left(\cos\left(\arcsin\left(\sin(\psi)/\rho\right) + \psi\right)\right) \\
&\quad \times \left(\sin\left(\arcsin\left(\sin(\psi)/\rho\right) + \psi\right)\right)^{m+n-2} \frac{\rho^{m+n-1}\,\mathrm{d}\rho}{\sqrt{\rho^2 - (\sin(\psi))^2}}\,.
\end{aligned}$$

Together with (3.3), this yields the claim. ∎

The relation between $f_{\ell,k}$ and $(\mathcal{R}_m f)_{\ell,k}$ given in Theorem 3.2 is well suited for the numerical implementation, see Section 4. For showing uniqueness of a solution, the following equivalent form will be more appropriate.

Lemma 3.3. *Let $f \in C_0^\infty(B_1(0))$ and let $f_{\ell,k}$ and $(\mathcal{R}_m f)_{\ell,k}$ be as* (3.1) *and* (3.2)*. Further, for every $(\ell,k) \in I(n)$ denote*

(a) $\hat{g}_{\ell,k}(t) \coloneqq |\mathbb{S}^{n-2}|^{-1}(1-t)^{-(n-2)/2}(\mathcal{R}_m f)_{\ell,k}(\arccos\sqrt{t})$*;*

(b) $\hat{f}_{\ell,k}(s) \coloneqq f_{\ell,k}\left(\sqrt{1-s}\right)/2$*;*

(c) $F_\ell(t,s) \coloneqq \sum_{\sigma=\pm1} \sigma^\ell \left(\sqrt{t} - \sigma\sqrt{t-s}\right)^{m+n-2} C_\ell^{(n-2)/2}\left(\frac{\sqrt{t}\sqrt{t-s}+\sigma(1-t)}{\sqrt{1-s}}\right)$.

Then $\hat{f}_{\ell,k}$ and $\hat{g}_{\ell,k}$ are related via:

$$\forall t \in [0,1]\colon \quad \hat{g}_{\ell,k}(t) = \int_0^t \hat{f}_{\ell,k}(s)\,\frac{F_\ell(t,s)}{\sqrt{t-s}}\,\mathrm{d}s\,. \tag{3.7}$$

Proof. Substituting $w \coloneqq \sin(\psi)$ in (3.5) and using the trigonometric sum and difference identities shows

$$\begin{aligned}
&\frac{1}{|\mathbb{S}^{n-2}|}(\mathcal{R}_m f)_{\ell,k}(\arcsin(w)) \\
&\qquad = w^{-m}\int_w^1 f_{\ell,k}(\rho)\rho^{m+n-2}\sum_{\sigma=\pm1}\sigma^\ell \sin\left(\arcsin\left(w/\rho\right)-\sigma\arcsin(w)\right)^{m+n-2} \\
&\qquad\qquad \times C_\ell^{(n-2)/2}\left(\cos\left(\arcsin\left(w/\rho\right)-\sigma\arcsin(w)\right)\right)\frac{\rho\,\mathrm{d}\rho}{\sqrt{\rho^2-w^2}} \\
&\qquad = w^{-m}\int_w^1 f_{\ell,k}(\rho)\rho^{m+n-2}\sum_{\sigma=\pm1}\sigma^\ell \left(w/\rho\sqrt{1-w^2}-\sigma w\sqrt{1-w^2/\rho^2}\right)^{m+n-2} \\
&\qquad\qquad \times C_\ell^{(n-2)/2}\left(\sqrt{1-w^2/\rho^2}\,\sqrt{1-w^2}+\sigma\, w^2/\rho\right)\frac{\rho\,\mathrm{d}\rho}{\sqrt{\rho^2-w^2}} \\
&\qquad = w^{n-2}\int_w^1 f_{\ell,k}(\rho)\sum_{\sigma=\pm1}\sigma^\ell \left(\sqrt{1-w^2}-\sigma\sqrt{\rho^2-w^2}\right)^{m+n-2} \\
&\qquad\qquad \times C_\ell^{(n-2)/2}\left(\frac{\sqrt{\rho^2-w^2}\sqrt{1-w^2}+\sigma w^2}{\rho}\right)\frac{\rho\,\mathrm{d}\rho}{\sqrt{\rho^2-w^2}}
\end{aligned}$$

Next we set $w=\sqrt{1-t}$ and make the substitution $\rho=\sqrt{1-s}$. Then we have $1-w^2=t$, $\rho^2-w^2=t-s$ and $\arcsin(w)=\arccos(\sqrt{t})$, which shows

$$\begin{aligned}
\frac{(1-t)^{-(n-2)/2}}{|\mathbb{S}^{n-2}|}(\mathcal{R}_m f)_{\ell,k}(\arccos(\sqrt{t})) &= \frac{1}{2}\int_0^t f_{\ell,k}(\sqrt{1-s}) \\
&\quad\times\sum_{\sigma=\pm1}\sigma^\ell\left(\sqrt{t}-\sigma\sqrt{t-s}\right)^{m+n-2} C_\ell^{(n-2)/2}\left(\frac{\sqrt{t}\sqrt{t-s}+\sigma(1-t)}{\sqrt{1-s}}\right)\frac{\mathrm{d}s}{\sqrt{t-s}}\,.
\end{aligned}$$

This together with (a)-(c) yields (3.7). □

3.2 Solution uniqueness

Any of the integral equations (3.7) is of generalized Abel type. Using the symmetry of the Gegenbauer polynomials, we see that $F_\ell(s,s) = 2\,s^{(m+n-2)/2}\,C_\ell^{(n-2)/2}\left(\sqrt{1-s}\right)$. Since the Gegenbauer polynomials have zeros in $[0,1]$, so has the function $s\mapsto F_\ell(s,s)$. Consequently, standard theorems on well-posedness do not apply to (3.7), because such results require a non-vanishing diagonal.

To investigate unique solvability of (3.7) (and, as consequence, of (3.5)), we derive a uniqueness result for generalized Abel equations of the form

$$\forall t\in[a,b]\colon\qquad \int_a^t \frac{F(t,s)}{\sqrt{t-s}}\,f(s)\,\mathrm{d}s = g(t)\,, \tag{3.8}$$

where $g\in C([a,b])$ corresponds to given data and $F\in C(\Delta(a,b))$, with $\Delta(a,b)\coloneqq\{(t,s)\in\mathbb{R}^2 \mid a\le s\le t\le b\}$, is a continuous kernel.

Theorem 3.4 (Solution uniqueness of Abel equations with kernel having zeros on the diagonal)**.** *Suppose that $F\colon \Delta(a,b) \to \mathbb{R}$, where $a < b$, satisfies the following:*

(F1) $F \in C^3(\Delta(a,b))$.

(F2) $N_F \coloneqq \{s \in [a,b) \mid F(s,s) = 0\}$ *is finite and consists of simple roots.*

(F3) For every $s \in N_F$, *the gradient* $(\beta_1, \beta_2) \coloneqq \nabla F(s,s)$ *satisfies*

$$1 + \frac{1}{2}\,\frac{\beta_1}{\beta_1 + \beta_2} > 0\,. \tag{3.9}$$

Then, for any $g \in C([a,b])$, *equation* (3.8) *has at most one solution* $f \in C([a,b])$.

Proof. See Appendix A. □

To the best of our knowledge, Theorem 3.4 is new; we are not aware of similar results for generalized Abel equations with zeros in the diagonal of the kernel. We derive this result by exploiting a well-posedness theorem due to Volterra and Pérès for first kind Volterra equations (see Lemma A.1) together with a standard procedure of reducing generalized Abel equations to Volterra integral equations of the first kind. We now apply Theorem 3.4 to the integral equation (3.7):

Theorem 3.5 (Uniqueness of recovering $f_{\ell,k}$)**.** *Suppose* $m > -(n+1)/2$. *For any* $f \in C_0^\infty(B_1(0))$ *and any* $(\ell,k) \in I(n)$, *the spherical harmonic coefficient* $f_{\ell,k}$ *of* f *can be recovered as the unique solution of*

$$\forall \psi \in (0,\pi/2)\colon \quad (\mathcal{R}_m f)_{\ell,k}(\psi) = |\mathbb{S}^{n-2}| \sin(\psi)^{-m} \int_{\sin(\psi)}^1 f_{\ell,k}(\rho) \frac{\rho\, K_\ell(\psi,\rho)\,\mathrm{d}\rho}{\sqrt{\rho^2 - (\sin(\psi))^2}}\,,$$

with the kernel functions K_ℓ *defined by* (3.6).

Proof. Let $f \in C_0^\infty(B_1(0))$ vanish outside a ball of Radius $1 - a^2$. According to Lemma 3.3, it is sufficient to show that (3.7) has a unique solution. To show that this is indeed the case, we apply Theorem 3.4 by verifying that $F_\ell\colon \Delta(a,1) \to \mathbb{R}$ satisfies conditions (F1)-(F3).

Ad (F1): Using the abbreviations $q \coloneqq m + n - 2$ and $C \coloneqq C_\ell^{(n-2)/2}$, the kernel F_ℓ can be written in the form

$$\forall (t,s) \in \Delta(a,1)\colon\ F_\ell(t,s) = \sum_{\sigma=\pm 1} \sigma^\ell \left(\sqrt{t} - \sigma\sqrt{t-s}\right)^q C\left(\frac{\sqrt{t}\sqrt{t-s} + \sigma(1-t)}{\sqrt{1-s}}\right).$$

From this expression it is clear that F_ℓ is smooth on $\{(t,s) \in \Delta(a,1) \mid t \neq s\}$. Further, by using $C(-x) = (-1)^\ell C(x)$ one sees that F_ℓ is an even polynomial in $\sqrt{t-s}$. This shows that F_ℓ is also smooth on the diagonal $\{(t,s) \in \Delta(a,1) \mid t = s\}$.

Ad (F2): Next, consider the restriction $v(s) \coloneqq F_\ell(s,s) = 2\,s^{q/2} C(\sqrt{1-s})$ of the kernel to the diagonal. As an orthogonal polynomial, C has a finite number of isolated and simple roots. We conclude that the same holds true for v.

Ad (F3): Let $s_0 \in [a,1)$ be a zero of v and set $(\beta_1,\beta_2) \coloneqq \nabla F_\ell(s_0,s_0)$. Then

$$\beta_1+\beta_2 = v'(s_0) = -\frac{s_0^{q/2}}{\sqrt{1-s_0}} C'\left(\sqrt{1-s_0}\right) . \tag{3.10}$$

Next we compute $\beta_1 = (\beta_1+\beta_2)-\beta_2$. We have

$$\begin{aligned}
F_\ell(s_0,s_0-\epsilon) &= \sum_{\sigma=\pm 1} \sigma^\ell \left(\sqrt{s_0}-\sigma\sqrt{\epsilon}\,\right)^q C\left(\frac{\sqrt{s_0}\sqrt{\epsilon}+\sigma(1-s_0)}{\sqrt{1-s_0+\epsilon}}\right) \\
&= \sum_{\sigma=\pm 1} \sigma^\ell \left(s_0^{q/2} - \sigma q s_0^{(q-1)/2}\sqrt{\epsilon} + \frac{q(q-1)}{2} s_0^{(q-2)/2}\epsilon\right) \\
&\quad \times \left(C'(\sigma\sqrt{1-s_0})\frac{\sqrt{s_0}}{\sqrt{1-s_0}}\sqrt{\epsilon} + \Big(C''(\sigma\sqrt{1-s_0})\frac{s_0}{2(1-s_0)} \right. \\
&\qquad\qquad \left. - \frac{\sigma}{\sqrt{1-s_0}} C'(\sigma\sqrt{1-s_0})\Big)\epsilon\right) + \mathcal{O}(\epsilon^2) \\
&= \frac{s_0^{q/2}}{\sqrt{1-s_0}}\left(-(2q+1)C'(\sqrt{1-s_0}) + \frac{s_0 C''(\sqrt{1-s_0})}{\sqrt{1-s_0}}\right)\epsilon + \mathcal{O}(\epsilon^2) .
\end{aligned}$$

Here for the last equality we used the symmetry properties $C'(-x) = (-1)^{\ell+1}C'(x)$ and $C''(-x) = (-1)^\ell C''(x)$ for the first and second derivatives of the Gegenbauer polynomials. Because C is a solution of the differential equation

$$(1-x^2)\,C''(x) - (n-1)\,x\,C'(x) + \ell\,(\ell+n-2)\,C(x) = 0$$

and s_0 is a zero of $t \mapsto C(\sqrt{1-t})$, we have the identity $s_0 C''(\sqrt{1-s_0})/\sqrt{1-s_0} = (n-1)C'(\sqrt{1-s_0})$. We conclude that $-\beta_2 = (-2q+n-2)\,s_0^{q/2}C'(\sqrt{1-s_0})/\sqrt{1-s_0}$. Together with (3.10) we obtain

$$\beta_1 = (-2q+n-3)\,\frac{s_0^{q/2}}{\sqrt{1-s_0}} C'(\sqrt{1-s_0}) . \tag{3.11}$$

From (3.10) and (3.11) it follows that

$$1+\frac{\beta_1}{2(\beta_1+\beta_2)} = 1+\frac{2q-n+3}{2} = m+\frac{n+1}{2} > 0 .$$

This shows (F3). Consequently, Theorem 3.4 implies that $\hat{f}_{\ell,k}$ is the unique solution of the integral equation (3.3). □

Theorem 3.5 immediately implies the following uniqueness result for the conical Radon transform $\mathcal{R}_m$.

Corollary 3.6 (Invertibility of $\mathcal{R}_m$)**.** *Suppose $m > -(n+1)/2$. If $f_1, f_2 \in C_0^\infty(B_1(0))$ are such that $\mathcal{R}_m f_1 = \mathcal{R}_m f_2$, then $f_1 = f_2$.*

Proof. Let $f \in C_0^\infty(B_1(0))$ satisfy $(\mathcal{R}_m f)_{\ell,k} = 0$ for all $(\ell,k) \in I(n)$. According to Theorem 3.5, the integral equation (3.5) has the unique solution $f_{\ell,k} = 0$, which implies $f = 0$. The linearity of $\mathcal{R}_m$ gives the claim. □

4 Numerical implementation

Theorems 3.2 and 3.5 are the basis of the following inversion method for the conical Radon transform $\mathcal{R}_m$:

(a) Compute the expansion coefficients $(\mathcal{R}_m f)_{\ell,k}$ in (3.2).

(b) Recover $f_{\ell,k}$ from $(\mathcal{R}_m f)_{\ell,k}$ by solving (3.5).

(c) Compute $f(r\theta) = \sum_{(\ell,k)\in I(n)} f_{\ell,k}(r) Y_{\ell,k}(\theta)$.

In this section, we show how to implement this reconstruction procedure. We restrict ourselves to two spatial dimensions ($n = 2$) and the case $m = 0$; extensions to general cases are straightforward.

4.1 Basic procedure for numerically inverting the conical Radon transform

In two spatial dimensions, the conical Radon transform with $m = 0$ can be written in the form

$$(\mathcal{R}f)(\varphi,\psi) \coloneqq \sum_{\sigma=\pm 1} \int_0^\infty f((\cos(\varphi),\sin(\varphi)) - r(\cos(\varphi-\sigma\psi),\sin(\varphi-\sigma\psi)))\,\mathrm{d}r\,. \tag{4.1}$$

Because $\mathcal{R}f$ consists of integrals of f over V-shaped lines, the 2D version is also known as the V-line Radon transform. In the 2D situation, the spherical harmonics expansion equals the common Fourier series expansion, and we obtain the following reconstruction procedure:

Algorithm 1 (Series expansion for inverting the V-line transform)**.**
Goal: Recover $f\colon \mathbb{R}^2 \to \mathbb{R}$ from the V-line transform $\mathcal{R}f\colon [0,2\pi]\times(0,\pi/2)\to\mathbb{R}$.

(S1) Compute $g_\ell(s) \coloneqq \int_0^{2\pi} (\mathcal{R}f)(\alpha,\arcsin(s)) e^{-i\alpha\ell}\,\mathrm{d}\alpha$.

(S2) For all $\ell\in\mathbb{Z}$, recover f_ℓ by solving the Abel equation

$$\forall s\in[0,1]\colon \quad g_\ell(s) = \int_s^1 f_\ell(\rho)\frac{\rho K_\ell(s,\rho)}{\sqrt{\rho^2-s^2}}\,\mathrm{d}\rho, \tag{4.2}$$

with $K_\ell(s,\rho) \coloneqq \sum_{\sigma=\pm1}\sigma^\ell \cos\left(\ell\left(\arcsin(s/\rho) - \sigma\arcsin(s)\right)\right)$.

(S3) Evaluate $f(r(\cos\alpha,\sin\alpha)) = \frac{1}{2\pi}\sum_{\ell\in\mathbb{Z}} f_\ell(\rho) e^{i\ell\alpha}$.

In order to implement Algorithm 1, we suppose that we have given discrete data

$$\mathbf{g}[k,i] \coloneqq \mathcal{R}_m f(\varphi_k,\arcsin(s_i)) \quad \text{for } (k,i)\in\{M/2,\dots,M/2-1\}\times\{0,\dots N\}\,.$$

Here $\varphi_k \coloneqq 2\pi(k-1)/M$ describe the discrete vertex positions and $s_i \coloneqq i/N$ for $i \in \{0,\dots,N\}$ corresponds to the discretization of the half opening angles. In our implementation, we discretize any step in Algorithm 1. For computing the Fourier coefficients in Step (S1) and for evaluating the Fourier series in Step (S3), we use the standard FFT algorithm. In Step (S1), the FFT algorithm outputs approximations to g_ℓ for $\ell \in \{-M/2, -M/2+1, \dots, M/2-1\}$, which are used as inputs for the second step. The main issue in the reconstruction procedure is implementing Step (S2), which consists in solving the integral equation (4.2). For that purpose we use product integration method using the mid-point rule [25, 34, 44], as outlined in the following subsection.

4.2 The mid-point method for numerically solving (4.2)

To apply the mid-point method to (4.2) for any $\ell \in \mathbb{Z}$, one starts with the uniform discretization $s_i = i/N$ of the interval $[0,1]$. Evaluating (4.2) at the discretization points yields

$$\forall i \in \{0,\dots,N\}\colon \quad g_\ell(s_i) = \sum_{j=i}^{n-1} \int_{s_j}^{s_{j+1}} f_\ell(\rho)\, \frac{\rho\, K_\ell(s_i,\rho)}{\sqrt{\rho^2 - s_i^2}}\, \mathrm{d}\rho\,. \tag{4.3}$$

One approximately evaluates the right hand side in (4.3) by replacing the restriction of $\rho \mapsto f_\ell(\rho)\, K_\ell(s_i,\rho)$ to $[s_j, s_{j+1}]$ by the function value at the mid-point of the interval and computing the resulting integral exactly. By setting $\rho_j \coloneqq (j+1/2)/N$, this yields

$$\begin{aligned} \forall i \in \{0,\dots,N\}\colon\ g_\ell(s_i) &\simeq \sum_{j=i}^{N-1} w_{i,j} K_\ell(s_i,\rho_j) f_\ell(\rho_j)\,, \\ w_{i,j} &\coloneqq \int_{s_j}^{sj+1} \frac{\rho}{\sqrt{\rho^2 - s_i^2}}\, \mathrm{d}\rho = \frac{\sqrt{(j+1)^2 - i^2} - \sqrt{j^2 - i^2}}{n}\,. \end{aligned} \tag{4.4}$$

The mid-point rule defines numerical approximations $\mathbf{f}_\ell[j] \simeq f_\ell(\rho_j)$ by requiring (4.4) to be exactly satisfied with $\mathbf{f}_\ell[j]$ instead of $f_\ell(\rho_j)$.

Next we define

(a) the discrete kernels $\mathbf{K}_\ell = (w_{i,j}\, K_\ell(s_i,\rho_j))_{i,j=0,\dots,N-1} \in \mathbb{R}^{N\times N}$;

(b) the discrete data $\mathbf{g}_\ell = (g_\ell(s_0),\dots,g_\ell(s_{N-1}))^\mathsf{T} \in \mathbb{R}^N$;

(c) the discrete unknowns $\mathbf{f}_\ell = (\mathbf{f}_\ell[0],\dots,\mathbf{f}_\ell[N-1])^\mathsf{T} \in \mathbb{R}^N$.

The product integration method using the composite mid-point rule consists in the end in solving the following system of linear equations:

$$\text{Find} \quad \mathbf{f}_\ell \in \mathbb{R}^N \quad \text{such that} \quad \mathbf{g}_\ell = \mathbf{K}_\ell\, \mathbf{f}_\ell\,. \tag{4.5}$$

The matrix $\mathbf{K}_\ell$ is triangular. Therefore, in the case that $\mathbf{K}_\ell$ is non-singular and well conditioned, equation (4.5) can efficiently be solved by forward substitution.

4.3 Regularization of the mid-point method

Because the kernel function K_ℓ has zeros in the diagonal, the matrix $\mathbf{K}_\ell$ may have diagonal entries being exactly or at least close to zero. As a consequence, solving the system (4.5) of linear equations is ill-conditioned. In order to obtain a stable solution, regularization methods have to be applied. We use the method of Tikhonov regularization for that purpose [10, 18, 20, 40]. In this approach, regularized solutions are defined as solutions of the regularized normal equation

$$\left(\mathbf{K}_\ell^\mathsf{T}\,\mathbf{K}_\ell + \lambda\,\mathbf{I}_N\right)\mathbf{f}_\ell = \mathbf{K}_\ell^\mathsf{T}\,\mathbf{g}_\ell\,. \tag{4.6}$$

Here $\mathbf{I}_N \in \mathbb{R}^{N\times N}$ is the identity matrix and $\lambda > 0$ is a regularization parameter.

The regularization parameter in (4.6) could be chosen in dependence on the index $\ell \in \{-M/2, -M/2+1, \ldots, M/2-1\}$, in combination with a data driven parameter selection rule. However, the development of such strategies is outside the scope of this paper. In our initial simulation presented below, we take the regularization parameter λ simply as a user selected constant. Nevertheless, we emphasize that λ has to be taken carefully as a trade of between stability of inverting $\mathbf{K}_\ell^\mathsf{T}\,\mathbf{K}_\ell + \lambda\,\mathbf{I}_N$ and accuracy of approximating the pseudo-inverse of $\mathbf{K}_\ell$. Tikhonov regularization can be interpreted as one member of filter based regularization methods based on singular value decomposition [10]. Instead of Tikhonov regularization, one could also use any other filter based regularization method for stabilizing the product integration method. For comparison purpose we also implemented truncated singular value decomposition (SVD) for regularizing (4.5).

For the case that the kernel is non-vanishing on the diagonal, the product integration method (4.5) using the mid-point rule is known to be convergent of order 3/2; see [44, Theorem 3.5]. Due to the zeros of the kernels, such results cannot be applied to the conical Radon transform. We are currently not aware of any results for the (regularized) product integration method in that direction. Such investigations is an interesting line of future research.

4.4 Numerical example

The reconstruction procedure outlined above has been implemented in MATLAB and tested on a discretized version of a Smiley phantom shown in Figure 2(a) sampled on a Cartesian 301×301 grid. For implementing the conical Radon transform, we numerically compute the integrals over V-lines using the composite trapezoidal rule. The numerically computed V-line transform $\mathbf{g} \in \mathbb{R}^{256\times 301}$ using $M = 256$ vertex positions and 301 opening angles is shown in Figure 2(b). The numerical reconstruction from such simulated data using Algorithm 1 is shown in Figure 2(c). The regularization parameter has been taken as $\lambda = 0.015$. We also tested our algorithm applied to noisy data $\mathbf{g} + \mathbf{z}$, where $\mathbf{z} \in \mathbb{R}^{256\times 301}$ is a realization of Gaussian white noise with $\|\mathbf{z}\|_{\ell^2}/\|\mathbf{g}\|_{\ell^2} \simeq 0.04$. For noisy data, $\lambda = 0.05$ turned out to be a suitable regularization parameter. In the resulting reconstruction, the structure of the phantom is still clearly visible, although the noise has been amplified. Strategies for further improving the reconstruction quality will be investigated in future work. Our numerical experiments using truncated SVD led to results very similar to Tikhonov regularization (not

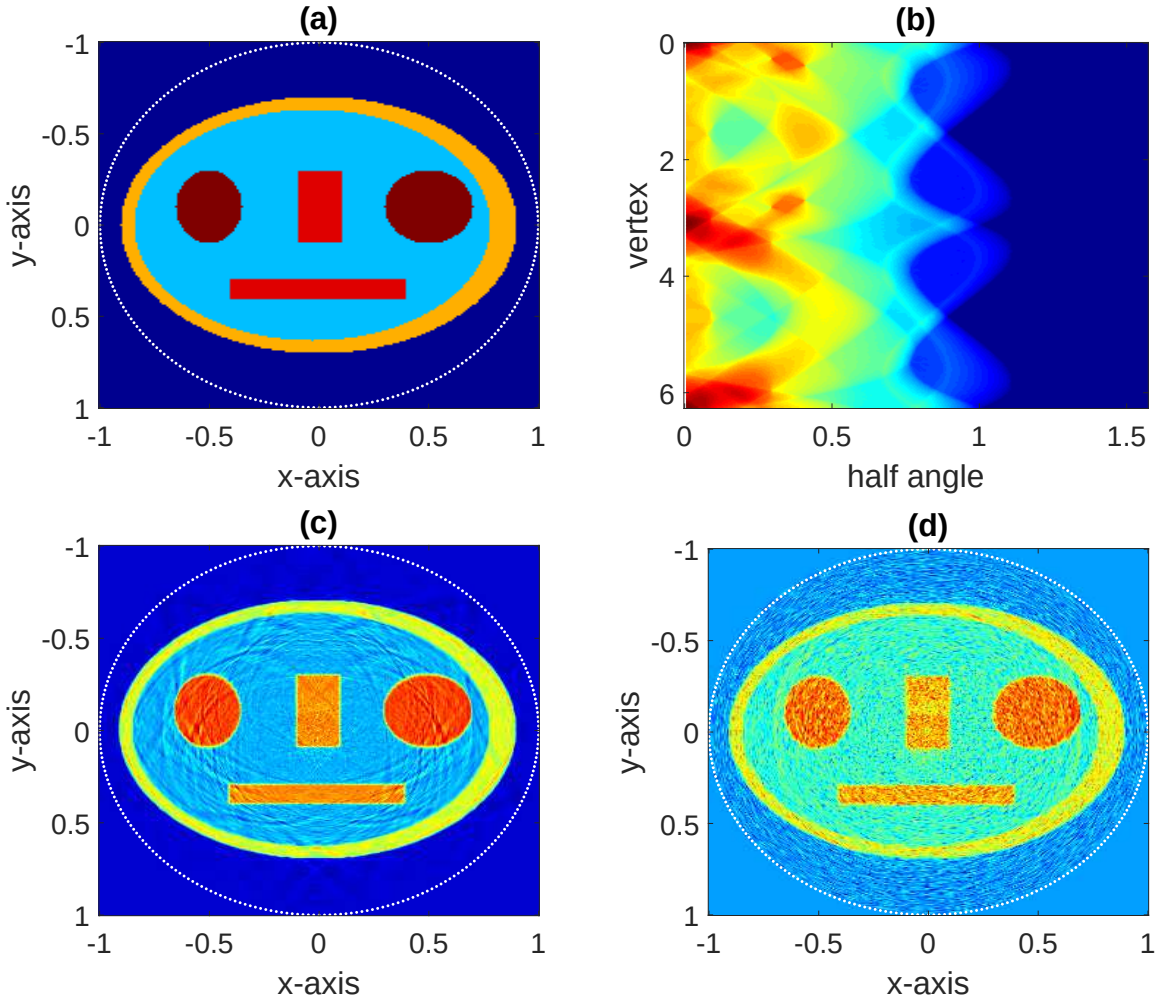

Figure 2: Reconstruction results: (a) Smiley phantom f. (b) Simulated conical Radon transform $\mathcal{R}f$. (c) Numerical reconstruction from simulated data using the derived algorithm. (d) Numerical reconstruction after adding Gaussian white noise with a relative ℓ^2-error of 4%.

displayed). We remark that Tikhonov regularization is numerically more efficient because it only requires solving one linear equation for a symmetric positive definite matrix.

5 Conclusion

In this paper we studied the conical Radon transform $\mathcal{R}_m$ that integrates a function in $\mathbb{R}^n$ over circular cones having vertices on a sphere and axis orthogonal to the sphere including a radial weight r^m. By exploiting the spherical symmetry of the problem, we have been able to decompose $\mathcal{R}_m$ in a product of explicitly computed one-dimensional integral equations of generalized Abel type. By analyzing the zeros on the diagonal of the kernels and exploiting a general uniqueness result developed in this paper, we have been able to show that any of

these integral equations has a unique solution (provided $m > -(n+1)/2$). This in particular implies the invertibility of $\mathcal{R}_m$.

Based on our analytic results, we developed a discrete reconstruction algorithm where the main step is the numerical solution of the Abel type equations involving the kernels K_ℓ. For that purpose, we applied the product integration method that yields to a linear matrix equation (4.5). Because of the zeros of $s \mapsto K_\ell(s,s)$, equation (4.5) is ill-conditioned and has to be regularized, which has been done by Tikhonov regularization. In future work we intend to investigate this issue by theoretically analyzing the degree of ill-posedness of the Abel integral equations with kernels K_ℓ and the stability of inverting $\mathcal{R}_m$. We thereby also will consider convergence properties of the (regularized) product integration method. Further, it would be interesting to characterize the range of the involved Abel integral operators which finally might lead to a characterization of the range of $\mathcal{R}_m$. Other interesting lines of research are considering the conical Radon transform with non-orthogonal axis or deriving similar results for the case where the vertices are restricted to a cylindrical surface.

A Uniqueness of Abel and first kind Volterra integral equations with kernels having zeros on the diagonal

In this appendix we prove Theorem 3.4, a uniqueness result for generalized Abel equation. For that purpose we first develop a uniqueness result for Volterra integral equations of the first kind (see Theorem A.2), that will subsequently be used to derive Theorem 3.4.

A.1 First kind Volterra integral equations

For kernel $V \in C(\Delta(a,b))$ and data $g\colon [a,b] \to \mathbb{R}$, we consider the Volterra integral equation of first kind,

$$\forall u \in [a,b]\colon \qquad \int_a^u V(u,s)\, f(s)\, \mathrm{d}s = g(u)\,. \tag{A.1}$$

Standard results guaranteeing existence and uniqueness of a solution of (A.1) require $V(s,s) \neq 0$ for all $s \in [a,b]$. Instead, we make use of the following non-standard result that yields solution uniqueness in the case that the kernel has zeros on the diagonal.

Lemma A.1 (Theorem of Volterra and Pérès)**.** *Equation* (A.1) *has exactly one solution* $f \in C([a,b])$ *if* V *and* g *satisfy the following:*

(a) $s \mapsto V(s,s)$ *has a simple root at* a*.*

(b) $V(s,s) \neq 0$ *for all* $s \in (a,b]$*.*

(c) There exist $p_k \in C(\Delta(a,b))$ *with* $\partial_1 p_k \in C(\Delta(a,b))$ *for* $k \in \{0,1,2\}$*, and* $\alpha_1, \alpha_2 \in \mathbb{R}$ *with* $\alpha_1 + \alpha_2 \neq 0$ *and* $1 + \alpha_1/(\alpha_1+\alpha_2) > 0$*, such that*

$$V(u,s) = \alpha_1(u-a) + \alpha_2(s-a) + \sum_{k=0}^{2} p_k(u,s)(s-a)^k(u-a)^{2-k}\,.$$

(d) $g(s) = (s-a)^2 h(s)$ *for some* $h \in C^1([a,b])$.

Proof. See [12, 43]. □

In the case that the kernel V has several zeros on the diagonal, we apply Lemma A.1 to derive the following Theorem A.2. There we only investigate uniqueness of solution, because in the exact data case the existence of a solution is always guaranteed. Attempting to characterizing the range of the forward operators is an important aspect, that will be addressed in future work.

Theorem A.2 (Uniqueness result for first kind Volterra integral equations having several zeros in the diagonal)**.** *Suppose that* $V\colon \Delta(a,b) \to \mathbb{R}$ *satisfies the following:*

(V1) $V \in C^3(\Delta(a,b))$.

(V2) $N_V \coloneqq \{s \in [a,b) \mid V(s,s) = 0\}$ *is finite and consists of simple roots.*

(V3) For every $s \in N_V$, $(\alpha_1, \alpha_2) \coloneqq \nabla V(s,s)$ *satisfies* $1 + \alpha_1/(\alpha_1 + \alpha_2) > 0$.

Then, for every $g \in C([a,b])$, (A.1) *has at most one solution* $f \in C([a,b])$.

Proof. Write $N_V = \{s_0, s_1, \dots, s_N\}$ with $s_0 < s_1 < \cdots < s_N$ and assume that $s_0 = a$. The case $s_0 > a$ can be treated in a similar manner after showing solution uniqueness on $[a, s_0]$ using the standard well-posedness result for non-vanishing diagonal. We will show recursively that f is uniquely determined on $[a, s_{i+1}]$ by (A.1) for $i = 0, \dots, N-1$. For $i = 0$, consider the first kind Volterra equation

$$\forall u \in [a, s_1]\colon \qquad \int_a^u V(u,s) f(s)\,\mathrm{d}s = g_1(u)\,, \tag{A.2}$$

where $g_1 \coloneqq g|[a,s_1]$. The assumptions made on V imply that $V|\Delta(a,b_1)$ satisfies the conditions (a)-(c) in Lemma A.1 for every $b_1 < s_1$. Consequently, Lemma A.1 implies that (A.2) uniquely determines $f|[a,b_1]$. Taking the limit $b_1 \to s_1$ and using the continuity of a possible solution shows that $f|[a,s_1]$ is uniquely defined. Now suppose that $f|[a,s_i]$ has already been shown to be uniquely determined and consider the integral equation $\int_{s_i}^u V(u,s) f(s)\,\mathrm{d}s = g_i(u)$ for $u \in [s_i, s_{i+1}]$, where $g_i(u) \coloneqq g(u) - \int_a^{s_i} V(u,s) f(s)\,\mathrm{d}s$. Lemma A.1 applied to the kernel $V|\Delta(s_i, b_{i+1})$ for $b_i \in (s_i, s_{i+1})$ and taking the limit $b_{i+1} \to s_{i+1}$ afterwards shows that $f|[a,s_{i+1}]$ is uniquely determined. □

A.2 Proof of Theorem 3.4

We now derive Theorem 3.4 as a consequence of Theorem A.2. For that purpose, suppose that $f \in C([a,b])$ is a solution of (3.8) with right hand side $g \in C([a,b])$ and kernel $F\colon \Delta(a,b) \to \mathbb{R}$ satisfying the assumptions (F1)-(F3) in Theorem 3.4. By multiplying (3.8) with $1/\sqrt{u-t}$, integrating over t and changing the order of integration, we obtain

$$\forall u \in [a,b]\colon \qquad \int_a^u \left(\int_s^u \frac{F(t,s)}{\sqrt{t-s}\sqrt{u-t}}\,\mathrm{d}t \right) f(s)\,\mathrm{d}s = \int_a^u \frac{g(t)}{\sqrt{u-t}}\,\mathrm{d}t\,. \tag{A.3}$$

The integral equation (A.3) is a particular case of(A.1) with continuous right hand side $u \mapsto \int_a^u g(t)/\sqrt{u-t}\,\mathrm{d}t$ and kernel V defined by

$$V(u,s) \coloneqq \int_s^u \frac{F(t,s)}{\sqrt{t-s}\sqrt{u-t}}\,\mathrm{d}t = \int_0^1 \frac{F(s+(u-s)r,s)}{\sqrt{r}\sqrt{1-r}}\,\mathrm{d}r\,.$$

Consequently, (3.8) has a unique solution if the kernel $V\colon \Delta(a,b) \to \mathbb{R}\colon (u,s) \mapsto V(u,s)$ satisfies Items (V1)-(V3) in Lemma (A.1).

- Ad (V1): Because $F \in C^3(\Delta(a,b))$, we have $V \in C^3(\Delta(a,b))$.
- Ad (V2): For any $t \in [a,b]$ we have $V(s,s) = F(s,s)\int_0^1 1/\sqrt{r(1-r)}\,\mathrm{d}r = \pi F(s,s)$. Consequently, $N_V = N_F$ is finite and only consists of simple roots.
- Ad (V3): Let s_0 be a root of $s \mapsto F(s,s)$ and let $(\beta_1,\beta_2) \coloneqq \nabla F(s_0,s_0)$ and $(\alpha_1,\alpha_2) \coloneqq \nabla V(s_0,s_0)$. Then $\alpha_1+\alpha_2 = \pi(\beta_1+\beta_2)$, and

$$\alpha_1 = \partial_1 V(s_0,s_0) = \int_0^1 \frac{[\partial_1 F(s+(u-s)r,s)]_{u=s=s_0}}{\sqrt{r}\sqrt{1-r}}\,\mathrm{d}r = \\ = \beta_1 \int_0^1 \frac{r}{\sqrt{r}\sqrt{1-r}}\,\mathrm{d}r = \frac{\pi}{2}\beta_1.$$

  We conclude that $1+\alpha_1/(\alpha_1+\alpha_2) = 1+\beta_1/(2\beta_1+2\beta_2)$, which is positive according to the assumptions made on the kernel F.

Consequently, Lemma A.1 implies that (A.3) has a unique solution, which implies the uniqueness of a solution of (3.8).

References

[1] M. Allmaras, D. Darrow, Y. Hristova, G. Kanschat, and P. Kuchment. Detecting small low emission radiating sources. *Inverse Probl. Imaging*, 7(1):47–79, 2013.

[2] G. Ambartsoumian, R. Gouia-Zarrad, and M. A. Lewis. Inversion of the circular Radon transform on an annulus. *Inverse Probl.*, 26(10):105015, 11, 2010.

[3] G. Ambartsoumian and S. Moon. A series formula for inversion of the V-line Radon transform in a disc. *Comput. Math. Appl.*, 66(9):1567–1572, 2013.

[4] G. Ambartsoumian and S. Roy. Numerical inversion of a broken ray transform arising in single scattering optical tomography. *IEEE Trans. Comput. Imaging*, 2(2):166–173, 2016.

[5] R. Basko, G. L. Zeng, and G. T. Gullberg. Analytical reconstruction formula for one-dimensional compton camera. *IEEE Trans. Nucl. Sci.*, 44(3):1342–1346, 1997.

[6] R. Basko, G. L. Zeng, and G. T. Gullberg. Application of spherical harmonics to image reconstruction for the compton camera. *Phys. Med. Biol.*, 43(4):887, 1998.

[7] A. M. Cormack. Representation of a function by its line integrals, with some radiological applications. *J. Appl. Phys.*, 34(9):2722–2727, 1963.

[8] M. J. Cree and P. J. Bones. Towards direct reconstruction from a gamma camera based on compton scattering. *IEEE Trans. Med. Imaging*, 13(2):398–407, 1994.

[9] S. R. R. Deans. Gegenbauer transforms via the Radon transform. *SIAM J. Math. Anal.*, 10(3):577–585, 1979.

[10] H. W. Engl, M. Hanke, and A. Neubauer. *Regularization of inverse problems*, volume 375 of *Mathematics and its Applications*. Kluwer Academic Publishers Group, Dordrecht, 1996.

[11] D. B. Everett, J. S. Fleming, R. W. Todd, and J. M. Nightingale. Gamma-radiation imaging system based on the compton effect. *Proc. IEEE*, 124(11):995–1000, 1977.

[12] S. Fenyö and H.-W. Stolle. *Theorie und Praxis der linearen Integralgleichungen 3*, volume 76 of *Lehrbücher und Monographien aus dem Gebiete der Exakten Wissenschaften (LMW). Mathematische Reihe*. Birkhäuser Verlag, Basel, 1984.

[13] D. Finch, M. Haltmeier, and Rakesh. Inversion of spherical means and the wave equation in even dimensions. *SIAM J. Appl. Math.*, 68(2):392–412, 2007.

[14] D. Finch, S. K. Patch, and Rakesh. Determining a function from its mean values over a family of spheres. *SIAM J. Math. Anal.*, 35(5):1213–1240, 2004.

[15] L. Florescu, V. Markel, and J. Schotland. Inversion formulas for the broken-ray Radon transform. *Inverse Probl.*, 27(2):025002, 13, 2011.

[16] L. Florescu, J. C. Schotland, and V. A. Markel. Single-scattering optical tomography. *Phys. Rev. E*, 79:036607, Mar 2009.

[17] Rim Gouia-Zarrad and Gaik Ambartsoumian. Exact inversion of the conical Radon transform with a fixed opening angle. *Inverse Probl.*, 30(4):045007, 12, 2014.

[18] C. W. Groetsch. *The Theory of Tikhonov Regularization for Fredholm Equations of the First Kind*. Pitman, Boston, 1984.

[19] M. Haltmeier. Exact reconstruction formulas for a radon transform over cones. *Inverse Probl.*, 30(3), 2014.

[20] P. C. Hansen. *Rank-Deficient and Discrete Ill-Posed Problems*. SIAM Monographs on Mathematical Modeling and Computation. SIAM, Philadelphia, PA, 1998.

[21] C. Jung and S. Moon. Inversion formulas for cone transforms arising in application of Compton cameras. *Inverse Probl.*, 31(1):015006, 20, 2015.

[22] C. Jung and S. Moon. Exact inversion of the cone transform arising in an application of a compton camera consisting of line detectors. *SIAM J. Imaging Sci.*, 9(2):520–536, 2016.

[23] P. Kuchment. *The Radon transform and medical imaging*. SIAM, Philadelphia, 2014.

[24] P. Kuchment and L. A. Kunyansky. Mathematics of thermoacoustic and photoacoustic tomography. *Eur. J. Appl. Math.*, 19:191–224, 2008.

[25] P. Linz. *Analytical and numerical methods for Volterra equations*, volume 7 of *SIAM Studies in Applied Mathematics*. SIAM, Philadelphia, PA, 1985.

[26] D. Ludwig. The Radon transform on euclidean space. *Comm. Pure Appl. Math.*, 19:49–81, 1966.

[27] V. Maxim, M. Frandeş, and R. Prost. Analytical inversion of the Compton transform using the full set of available projections. *Inverse Probl.*, 25(9):095001, 21, 2009.

[28] S. Moon. On the determination of a function from its conical radon transform with a fixed central axis. *SIAM J. Math. Anal.*, 48(3):1833–1847, 2016.

[29] M. Morvidone, M. K. Nguyen, T. T. Truong, and H. Zaidi. On the V-line Radon transform and its imaging applications. *Int. J. Biomed. Imaging*, 2010:208179, 6, 2010.

[30] C. Müller. *Spherical Harmonics*. Lecture Notes in Mathematics. Springer Verlag, Berlin-New York, 1966.

[31] F. Natterer. *The Mathematics of Computerized Tomography*, volume 32 of *Classics in Applied Mathematics*. SIAM, Philadelphia, 2001.

[32] M. K. Nguyen, T. T. Truong, and P. Grangeat. Radon transforms on a class of cones with fixed axis direction. *J. Phys. A*, 38(37):8003–8015, 2005.

[33] L. C. Parra. Reconstruction of cone-beam projections from compton scattered data. *IEEE Trans. Nucl. Sci.*, 47(4):1543–1550, 2000.

[34] R. Plato. The regularizing properties of the composite trapezoidal method for weakly singular Volterra integral equations of the first kind. *Adv. Comput. Math.*, 36(2):331–351, 2012.

[35] E. T. Quinto. The invertibility of rotation invariant Radon transforms. *J. Math. Anal. Appl.*, 91(2):510–522, 1983.

[36] R. T. Seeley. Spherical harmonics. *Amer. Math. Monthly*, 73(4):115–121, 1966.

[37] M. Singh. An electronically collimated gamma camera for single photon emission computed tomography. part I: Theoretical considerations and design criteria. *Med. Phys.*, 10(421):1983, 1983.

[38] B. Smith. Reconstruction methods and completeness conditions for two compton data models. *J. Opt. Soc. Am. A*, 22(3):445–459, 2005.

[39] F. Terzioglu. Some inversion formulas for the cone transform. *Inverse Probl.*, 31(11):115010, 21, 2015.

[40] A. N. Tikhonov and V. Y. Arsenin. *Solutions of Ill-Posed Problems*. John Wiley & Sons, Washington, D.C., 1977.

[41] R. W. Todd, J. M. Nightingale, and D. B. Everett. A proposed gamma camera. *Nature*, 251:132–134, 1974.

[42] T. Tomitani and M. Hirasawa. Image reconstruction from limited angle compton camera data. *Phys. Med. Biol.*, 47(12):2129, 2002.

[43] V. Volterra and J. Pérès. *Théorie générale des fonctionnelles*, volume 1. Gauthier-Villars, 1936.

[44] R. Weiss and R. S. Anderssen. A product integration method for a class of singular first kind Volterra equations. *Numer. Math.*, 18:442–456, 1971.